Middle and upper thermospheric odd nitrogen: 1. A new analysis of rocket data

David E. Siskind, J. M. Picone, and M. H. Stevens
E. O. Hulburt Center for Space Research, Naval Research Laboratory, Washington, DC, USA

K. Minschwaner
Department of Physics, New Mexico Institute of Mining and Technology, Socorro, New Mexico, USA

Received 17 March 2003; revised 10 October 2003; accepted 7 November 2003; published 17 January 2004.

[1] We evaluate the NRLMSISE-00 model for calculations of odd nitrogen (NO, N(^4S)) in the middle to upper thermosphere (z = 140–250 km). NRLMSISE-00 incorporates new data on O_2 that improves the agreement between odd nitrogen models and data significantly. In particular, the photochemical calculation that uses NRLMSISE-00 predicts a NO solar cycle variation that is significantly less than previous calculations and that agrees well with the NO observations. This agreement is consistent with the inference from FUV solar occultation data that the O_2 abundance above 140 km varies weakly with solar activity and that the O_2 vertical profile at solar maximum is sensitive to other factors besides molecular diffusion. Residual discrepancies remain with the comparison of calculated to observed N(^4S), which may be due to a combination of theoretical deficiencies and uncertainties in the observations. *INDEX TERMS:* 0355 Atmospheric Composition and Structure: Thermosphere—composition and chemistry; 0358 Atmospheric Composition and Structure: Thermosphere—energy deposition; 0310 Atmospheric Composition and Structure: Airglow and aurora; *KEYWORDS:* nitric oxide, thermosphere, UV spectroscopy, molecular oxygen, atomic nitrogen

Citation: Siskind, D. E., J. M. Picone, M. H. Stevens, and K. Minschwaner (2004), Middle and upper thermospheric odd nitrogen: 1. A new analysis of rocket data, *J. Geophys. Res.*, *109*, A01303, doi:10.1029/2003JA009943.

1. Introduction

[2] *Siskind and Rusch* [1992] (hereinafter referred to as SR92) first described the surprising difficulties in producing an accurate model of nitric oxide in the middle to upper thermosphere (z > 140 km). This altitude range is of interest because it includes the region where NO dominates the infrared cooling of the atmosphere [*Roble et al.*, 1987, Figure 8]. The modeling difficulties arose from a changed recommendation by the Jet Propulsion Laboratory (JPL) chemical kinetics evaluation panel [*DeMore et al.*, 1990] (hereinafter referred to as JPL90) for the temperature dependence of the reaction

$$N(^4S) + O_2 \rightarrow NO + O. \quad (1)$$

This reaction is slow at room temperatures, but the rate increases rapidly with increasing temperature. At thermospheric altitudes above 120 km, where the ambient temperature generally exceeds 400 K, reaction (1) becomes an important source of nitric oxide. The JPL90 recommendation increased the temperature sensitivity of reaction (1) which, when included in a photochemical model, significantly increased the calculated abundance of nitric oxide. As discussed by SR92, the calculated NO exceeded the observations by up to a factor of 3 at 200 km.

0148-0227/04/2003JA009943$09.00

[3] Such a discrepancy is surprising because in the middle to upper thermosphere, NO chemistry is thought to be quite simple. In addition to reaction (1), the only other source of NO is

$$N(^2D) + O_2 \rightarrow NO + O. \quad (2)$$

For temperatures near 300 K, equation (2) is much faster than reaction (1) and thus reaction (2) is the dominant source of NO where temperatures are relatively low, such as the mesosphere and lower thermosphere. The loss of NO is governed by the reaction

$$NO + N(^4S) \rightarrow N_2 + O. \quad (3)$$

Thus a simplified chemical equilibrium for NO can be defined as

$$[NO]_{eq} = \frac{(k_2 N(^2D) + k_1 N(^4S))O_2}{k_3 N(^4S)}, \quad (4)$$

where the k_is refer to the reaction rate coefficients of reactions (1)–(3). The abundance of N(^2D) can be difficult to assess and requires quantification of the processes which dissociate N_2 [see, e.g., *Siskind et al.*, 1995]. However, at higher altitudes reaction (2) becomes less important relative to reaction (1), particularly at high levels of solar activity. As discussed by SR92, for temperatures over 1000 K, the

Table 1. Summary of Published NO Measurements for $z > 150$ km and Solar Maximum Conditions

Reference	Date	Location		Daily Observed $F_{10.7}$	81-Day Averaged $F_{10.7}$	*Ap*
		Latitude, °N	Longitude, °W			
McCoy [1983]	8 Nov. 1979	32	106	292	221	12
Siskind et al. [1990]	9 Nov. 1981	32	106	237	216	4
Ogawa et al. [1984]	7 Sept. 1981	31	131	259	223	5

$N(^4S)$ source accounts for about 80% of the total NO production. In this case, to an accuracy of about 20%, equation (4) reduces to

$$NO = (k_1/k_3)O_2. \quad (5)$$

[4] Given this apparent simplicity, there are not many options for modifying the model to get an improved fit with the observations. *Siskind and Rusch* [1992] surveyed the literature and concluded that the faster temperature dependence for reaction (1) was supported by the laboratory data. They then proposed that reaction (3) was temperature-dependent in such a way that it increased for higher temperatures so as to compensate for the increased high-temperature production and keep the model NO from becoming overly large. One complication with this suggestion is that both reactions (1) and (3) serve as losses for $N(^4S)$. Increasing the rates of reactions (1) and (3) reduced the model $N(^4S)$ so that it was almost an order of magnitude less than the rocket data of *McCoy* [1983]. More recently, *Michael and Lim* [1992] and *Wennberg et al.* [1994] have remeasured the rate of reaction (3). Although neither study specifically considered temperatures near 500–1000 K that would be most relevant for our analysis, for the range of temperature they did consider (213–369 K [*Wennberg et al.*, 1994] and 1251–3152 K [*Michael and Lim*, 1992]), they found no evidence for the kind of temperature sensitivity proposed by SR92.

[5] Since SR92, the neutral atmospheric model (the Mass Spectrometer and Incoherent Scatter, or MSIS, model) that is used as an input to the photochemical calculations model has been upgraded [*Picone et al.*, 2002]. One change is that the new version of MSIS, called NRLMSISE-00 (hereinafter referred to as NRLMSIS), accounts for new data on the molecular oxygen number density $[O_2]$. As we will discuss, these new data appear to offer a solution to the problem posed by SR92 without requiring any modifications to the existing set of reactions and without degrading the model fit to the *McCoy* [1983] $N(^4S)$ data.

[6] In section 2 of this paper, we briefly review the NO data used. Most of this was discussed by SR92; however, we have also analyzed a new data set, that of *Cleary et al.* [1995], which was unavailable at the time of the earlier paper. All the data discussed in this paper come from sounding rockets; satellite data are presented by *Minschwaner et al.* [2003] (hereinafter referred to as Paper 2) and show results consistent with ours. In section 3, we review the NRLMSIS model with emphasis on the changed predictions for $[O_2]$. In section 4, we compare the NO and $N(^4S)$ data with the model using both NRLMSIS and the MSISE-90 model (hereinafter referred to as MSIS90) of *Hedin* [1991]. In section 5, we briefly explore some uncertainties and consequences of our work and section 6 is a summary.

2. NO Data

[7] In this section we summarize the data that were used to validate the model. As we noted in SR92, there are only three measurements of NO above 150 km for the highest levels ($F_{10.7} > 200$) of solar activity. These are summarized in Table 1. SR92 also used a series of measurements made by the University of Tokyo group which were made at the same place and same local time, but spanned a range of solar activity levels. These are summarized in Table 2. Finally, we use two new measurements of high-altitude NO that were not available for the previous paper. These come from the Middle Ultraviolet Spectral Analysis of Nitrogen Gases (MUSTANG) experiment [*Cleary et al.*, 1995]. The MUSTANG data have been used in several studies of thermospheric aeronomy [*Cleary et al.*, 1995; *Bucsela et al.*, 1998; *Hill et al.*, 2000]; however, to date the nitric oxide vertical profiles from that experiment have not been presented. Thus we will present some more detail on how that data were analyzed.

[8] MUSTANG was a rocket-borne ultraviolet (UV) spectrograph that flew from White Sands Missile Range on two occasions: 30 March 1990 and 19 March 1992. The most extensively studied data have been from the downleg of the 1992 flight [*Hill et al.*, 2000]. Since good NO data were also taken on the 1990 flight, we will also present a profile from the upleg data of that flight. Both the 1990 and 1992 flights occurred at the same time of day (morning) during similar levels of solar activity ($F_{10.7} = 186$ and 166 respectively) but for drastically different levels of geomagnetic activity ($Ap = 69$ and 4, respectively). The MUSTANG data are unique in that they represent the only high-quality NO data which extend above 200 km for conditions other than solar minimum [i.e., *Cravens*, 1981].

Table 2. Solar Cycle Variation of Middle Thermospheric NO: Summary of Rocket Observations

Reference	Date	Location		Daily Observed $F_{10.7}$	81-Day Averaged $F_{10.7}$	*Ap*
		Latitude, °N	Longitude, °W			
Ogawa et al. [1984]	7 Sept. 1981	31	131	259	223	5
Iwagami and Ogawa [1987]	25 Sept. 1982	31	131	168	162	13
Iwagami and Ogawa [1987]	16 Sept. 1983	31	131	105	115	26
Kita et al. [1988]	15 Jan. 1987	31	131	74	73	5

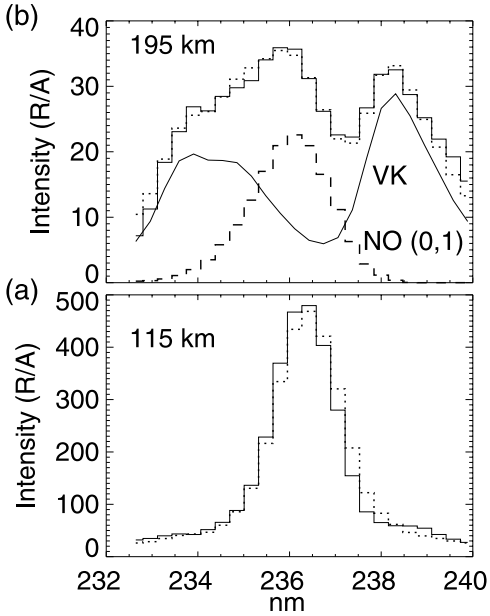

Figure 1. UV spectrum from the MUSTANG rocket of *Cleary et al.* [1995]. The data were taken on the downleg of the 19 March 1992 flight. The solid line is the data and the dotted line is the theoretical fit. (a) 115 km; the signal is almost entirely from NO. (b) 195 km; both NO (long-dashed curve) and N_2 Vegard Kaplan (dash-triple-dotted curve) contribute, and their relative contributions to the theoretical fit are shown separately.

[9] In the 1992 flight, MUSTANG observed the dayglow from 180 to 340 nm and as shown by *Cleary et al.* [1995], NO emission dominates the spectrum for $\lambda < 250$ nm. Additional emissions from the N_2 (A-X) Vegard Kaplan (VK) system, O^+ (247.0 nm) and N^+ (214.3 nm) are also present. To derive the NO densities, we used the NO $\gamma(0, 1)$ emission, centered near 237 nm. This band is bright enough to have high signal-to-noise up to and above 200 km; moreover, because it does not connect to the ground state vibrational level, it remains optically thin at all thermospheric altitudes [e.g., *Eparvier and Barth*, 1992]. We modeled its detailed rotational structure using the code of *Stevens* [1995] and obtained an emission rate factor (also known as "g-factor") of 2.53×10^{-6} photons/s molecule at 400 K. Paper 2 contains a more extensive discussion of the emission rate factor calculation and possible sources of uncertainty. Our emission rate factor was calculated for a representative solar flux appropriate with an $F_{10.7}$ value of 90. This could introduce a 2–3% underestimate of the emission rate factors at solar maximum. We inputted a temperature profile from the NRLMSIS model and convolved the calculated line-by-line spectrum with the 1 nm wide (FWHM) instrument slit function. Above about 140 km, the (0, 1) band blends with the VK(0, 3) and VK(1, 4) band. The rotational envelopes of the VK bands are taken from the AURIC radiance code [*Strickland et al.*, 1999] and simultaneously fit to the spectra with the NO(0, 1) band using standard multiple linear regression techniques (the IDL routine REGRESS [see also *Bevington*, 1969]). Figure 1 shows spectra for 115 km (the lowest altitude, Figure 1a) and 195 km (Figure 1b), with the theoretical fits. At 115 km, the signal is almost entirely from the NO; at 195 km, the contributions from the VK and NO are shown separately.

[10] Figure 2 shows the inferred NO slant column density (Figure 2a) and number density (Figure 2b) for both the 1992 and 1990 data. The slant column density is the scale factor used to fit the synthetic spectrum to the observed spectrum. [e.g., *Cleary*, 1986, equation (1)]. Implicit in this simple scaling is the assumption that the emission can be modeled by a single path-weighted temperature. Since the temperature is increasing rapidly with increasing altitude over much of the altitude range sampled by the rocket, the path-length-weighted temperature along the 90° viewing angle is somewhat greater than the temperature at the rocket altitude. Based upon calculations of the line of sight contribution function, we used a mean temperature equal to that given by the MSIS model for 5 km above the rocket altitude and estimate the error from this assumption to be 2–5% between 115 and 150 km and <2% above 150 km. We also tested the accuracy of our spectral fit by repeating the fit with another wavelength region from 220–230 nm which contains the NO $\gamma(0, 0)$, $\gamma(1, 1)$, and $\gamma(2, 2)$ bands. Our inferred slant column density with these bands as compared to that with the (0, 1) band varied from 10% greater between 115–140 km to 10% less at 200 km. Assuming these two errors are independent, the rms represents our assessment of the net systematic error in the spectral fit to the data, generally less than 10% at all altitudes.

[11] The number density (Figure 2b) is obtained by a simple onion peel inversion [*McCoy*, 1983] unconstrained by any smoothing or filtering. As a result, the lower-signal 1992 profile shows noise above 180 km that more sophisticated inversion techniques could undoubtedly suppress.

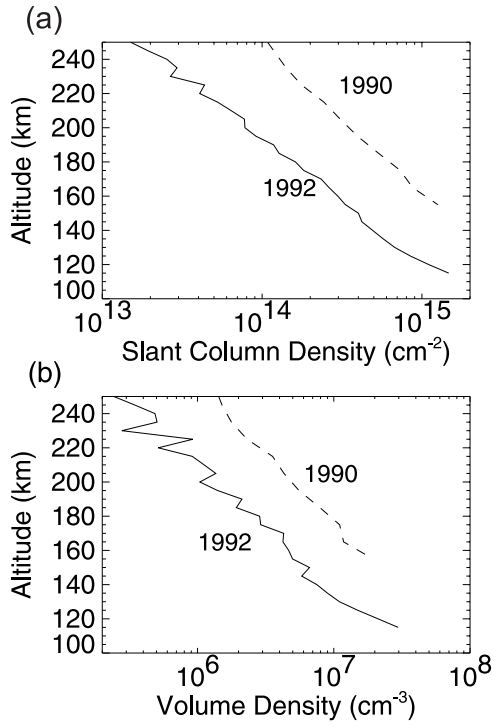

Figure 2. NO data inferred from the fits to the MUSTANG spectra (a) column density along the horizontal line of sight (b) number density.

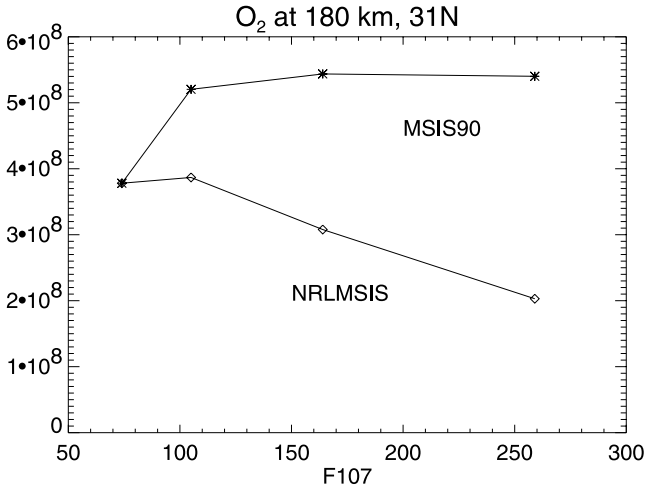

Figure 3. O_2 variation from NRLMSIS (diamonds) and MSIS90 (stars). The points are for the location, dates, and times of the University of Tokyo NO rocket campaign summarized in Table 2 and represent the empirical model input to the NO photochemical model.

Nonetheless, as we will show, this simplistic approach is adequate for comparing with the various models described below.

3. Description of the Models

3.1. 1-D NO_x Photochemical Transport Model (NOX1DIM)

[12] The model we use to compare with the rocket NO data is a one dimensional photochemical transport model (NOX1DIM) which has a long history of use [*Siskind et al.*, 1990; *Siskind and Rusch*, 1992; *Siskind et al.*, 1995]. The model calculates the vertical profile of NO, $N(^4S)$, and $N(^2D)$ and the ionic species (NO^+, O_2^+, N_2^+, O^+, N^+, and $O^+(^2D)$). Molecular and eddy diffusion are included for the NO and $N(^4S)$ calculations while photochemical equilibrium is assumed for the other species. The reaction rate set for the model has been discussed by *Siskind et al.* [1995] and SR92; specifically for the two sources of NO, reactions (1) and (2), we use $k_1 = 1.5 \times 10^{-11} e^{-3600/T}$ and $k_2 = 6 \times 10^{-12}$ cm^{-3} s^{-1}. Recently, new estimates for reaction (2) have been proposed, the effect of these proposals are discussed in section 5.

[13] The model results are also sensitive to various input parameters, most notably the neutral atmosphere, the solar spectrum and various cross sections used to calculate photoelectron ionization/dissociation. *Siskind et al.* [1995] discuss the latter two factors; these are most important for modeling NO in the relatively cooler lower thermosphere where $N(^2D)$ is the dominant NO source. Here where we consider NO above 140 km, the neutral atmosphere is the most important consideration. The model uses the temperature and density profiles from the MSIS-class empirical models which have undergone important revisions over the past two decades [see *Picone et al.*, 2002; *Hedin*, 1991, and references therein]. Some of these revisions are critical for present work and will be discussed in section 3.2. However, the general operation of the MSIS model and its use by NOX1DIM has remained the same. Both MSIS models use both the daily 10.7 cm solar flux ($F_{10.7}$) and the 81-day averaged $F_{10.7}$ as indicators of solar activity and the *Ap* index of geomagnetic activity. Each MSIS model is first run to produce 24 profiles of temperature, O, O_2, and N_2 densities at 1 hour intervals. These profiles are called by NOX1DIM for each model hour. NOX1DIM is run for several repeating model days to insure a diurnally reproducible solution. Also, based upon data from the Atmospheric Explorer C, D and E and Dynamics Explorer B, the MSIS models include $N(^4S)$ as one of the predicted constituents [*Hedin*, 1987]. The MSIS $N(^4S)$ will be compared with the calculated $N(^4S)$ from NOX1DIM to provide an additional test of the photochemical theory. Thus we will use the MSIS models both as an input to NOX1DIM (the O, O_2, N_2 and T) and test of NOX1DIM (the $N(^4S)$).

3.2. O_2 and the NRLMSIS Model

[14] From reactions (1)–(3), it is clear that two critical parameters are the O_2 concentration and the temperature, which is important for calculating the reaction rate coefficients. Of these, the O_2 density is one of the more uncertain parameters in MSIS models. NRLMSIS includes a significantly reformulated representation of thermospheric O_2; specifically, the underlying database now includes O_2 density data derived from the occultation of solar UV emissions observed by the Solar Maximum Mission (SMM) satellite [*Aikin et al.*, 1993]. In general, these new data do not agree well with the mass spectrometer data used in the older MSIS90 model which extrapolates low solar activity mass spectrometer data to higher $F_{10.7}$ values by assuming diffusive equilibrium. Specifically, for altitudes between 140–220 km, the NRLMSIS O_2 profiles fall below the MSIS90 profiles by an amount which increases with altitude and solar activity. Figure 3 shows the O_2 solar cycle variation for a midlatitude site which corresponds to the University of Tokyo's rocket campaign to measure NO (see Table 2). Thus Figure 3 portrays the O_2 which is used as an input to NOX1DIM in modeling the rocket NO measurements. The O_2 from MSIS90 generally increases with greater solar activity, consistent with the constraint of diffusive equilibrium, while the NRLMSIS O_2 is a factor of 2.5 less at the highest level of solar activity. Given the linear relationship between NO and O_2 at this altitude, we find this change to have a significant effect on model NO_x. This is shown in the next section.

4. NO_x Model/Data Comparisons

4.1. NO

[15] Figures 4 and 5 are updates to Figures 3 and 4 of SR92, respectively. Figure 4 compares each of the 3 rocket NO profiles with two photochemical calculations; one which uses NRLMSIS as an input and one which uses MSIS90 as an input. For all three rocket data sets, the model which uses NRLMSIS is clearly in the best agreement. Figure 5 shows the solar cycle variation of NO at 140 and 180 km. The data indicate a solar cycle variation of about a factor of 2–3 at 140 and 180 km. Owing to the large temperature change between solar minimum and maximum, the NOX1DIM calculation that uses MSIS90 predicts a much larger solar cycle change than is observed. Using

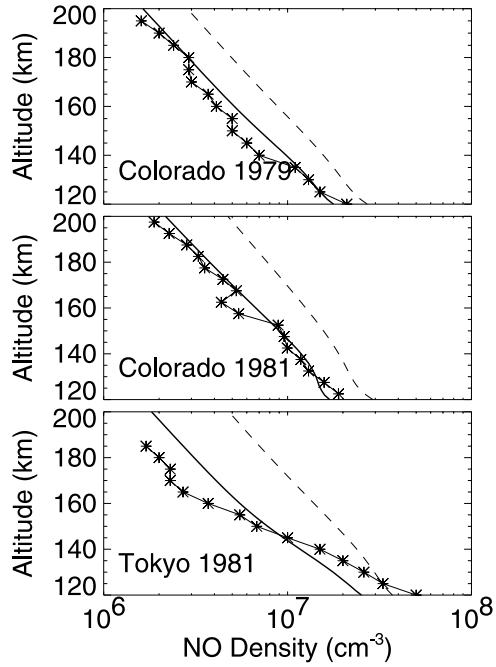

Figure 4. Comparison of calculated NO for several rocket profiles. The solid lines with stars are the data, the bold lines without stars are NOX1DIM using NRLMSIS as input, and the dashed lines are NOX1DIM using MSIS90 as input.

NRLMSIS as input gives an O_2 variation which partially counteracts the large temperature change (see Figure 3) and gives a calculated NO which is generally good agreement with the data.

[16] Figure 6 compares NOX1DIM to the two MUSTANG profiles. Since the MUSTANG data extend above 200 km, we show the calculated NO up to 250 km, which is the effective upper limit of the photochemical model. Although the data, particularly in 1992, become noisy above 200 km, several conclusions are apparent. First, as with the other 3 rocket flights, the photochemical model which uses NRLMSIS is obviously much better than that using MSIS90. Second, the comparison between NOX1DIM and the data for the 1990 is excellent while for 1992, even with NRLMSIS, the agreement is less good with NOX1DIM overestimating the data by about a factor of 1.5–2. Thus while the data indicate a factor of 3–4 change in NO in the 180–220 km region between high and low geomagnetic activity, the NOX1DIM only predicts a factor of 2 change. This may suggest that the actual O_2 density was even lower than that predicted by NRLMSIS.

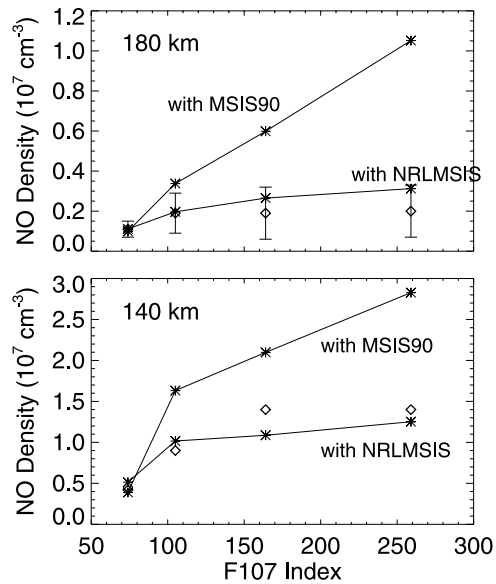

Figure 5. Solar cycle variation of NO from NOX1DIM using the indicated MSIS models (solid lines with stars). The data are summarized in Table 2 and are presented by the diamonds. The error bars at 180 km are from *Kuze and Ogawa* [1988, Figure 1].

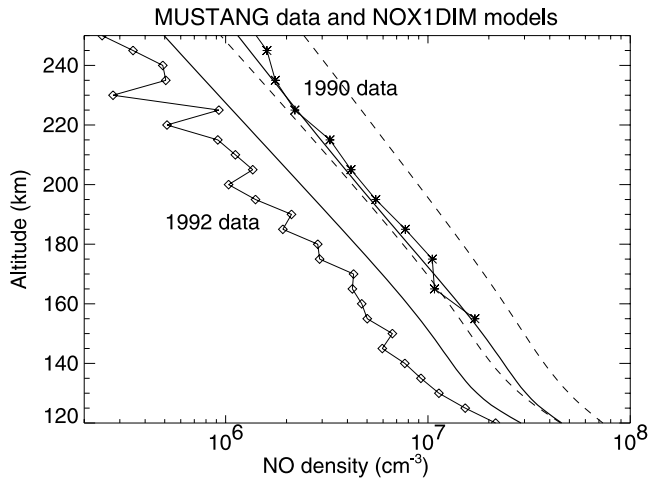

Figure 6. Comparison of calculated NO with MUSTANG rocket data for both the 30 March 1990 and 19 March 1992 flights. The 1992 data are the solid line with diamonds, and the 1990 data are the solid line with stars. The bold lines are NOX1DIM calculations which use NRLMSIS as input; the thin dashed curves are the NOX1DIM using MSIS90 as input. The rightmost pair of NOX1DIM curves correspond to the 1990 data; the leftmost pair correspond to the 1992 data.

[17] Uncertainties in the above analysis are mitigated by the analysis of the airglow that MUSTANG measured on this flight [*Bucsela et al.*, 1998]. For example, a colder atmosphere than predicted by NRLMSIS would lead to an overestimate of the data by NOX1DIM; however, *Bucsela et al.* [1998] found little evidence of large deviations from the MSIS predictions. Furthermore, the emissions selected for analysis by *Bucsela et al.* [1998] do not place strong constraints on the O_2 density. Finally, the generally good agreement achieved by *Bucsela et al.*'s [1998] model of the airglow data argues against any systematic error in the MUSTANG calibration (which was measured both before and after each flight [*Cleary et al.*, 1995]) Despite this residual uncertainly, it is clear that the NRLMSIS model yields superior agreement with the NO data for both rocket flights.

4.2. N(^4S)

[18] SR92 also presented photochemical model calculations of N(^4S) and compared them with the observation of

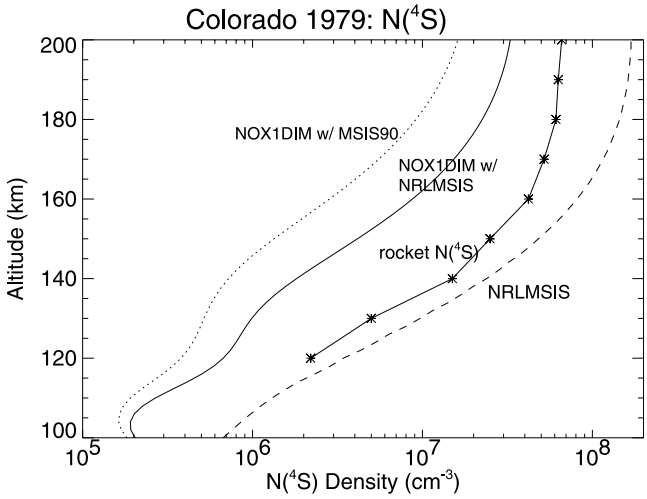

Figure 7. N(^4S) from two NOX1DIM calculations (solid line, NRLMSIS used as input; dotted line, MSIS90 used as input) compared with *McCoy* [1983] rocket data (solid line with stars) and from MSIS prediction (dashed line) for the same date, location, and time.

McCoy [1983]. The problem SR92 encountered was that the model which improved the agreement with the mid-upper thermospheric NO worsened the agreement with the N(^4S) data. Figure 7 shows that the use of the lower O_2 densities in NRLMSIS is likely a better solution to the problem. It compares the N(^4S) calculated by NOX1DIM with the McCoy data as well as the N(^4S) from the NRLMSIS model itself. Since the reactions of N(^4S) with O_2 and NO are the dominant losses for N(^4S), the NRLMSIS-based photochemical calculation, with its lower input O_2 and lower output NO will naturally yield more N(^4S). The photochemical model using MSIS90 is 10X less than that given by the empirical model at 200 km and over an order of magnitude less than at 140 km. Using NRLMSIS to drive NOX1DIM yields a factor of two increase in the calculated N(^4S) at all altitudes, relative to using MSIS90 as an input. While still significantly lower than the empirical N(^4S), this is an improvement.

[19] While the photochemical model deficit relative to the McCoy data is significant, even with NRLMSIS as an input, it is nonetheless still interesting that the McCoy data is a factor of 2–3 less than the MSIS prediction (note: the N(^4S) from NRLMSIS and MSIS90 are essentially identical and we do not distinguish between the two here). Figure 7 is consistent with a recent analysis by *Bishop and Feldman* [2003]. Using FUV emission data from the Hopkins Ultraviolet Telescope they concluded that MSIS [N(^4S)] predictions were a factor of 3 too large at high ($F_{10.7} > 200$) levels of solar activity. As Bishop and Feldman note, the MSIS predictions for high levels of solar activity are essentially extrapolations from the AE-C and AE-E databases. Although they deemed it unlikely that there could be a factor of 3 discrepancy in the MSIS [N] predictions, our result is consistent with their result. Thus some of the discrepancy between the NOX1DIM calculation and the NRLMSIS representation could be due to NRLMSIS.

[20] The remaining (and still large) discrepancy between the rocket data and NOX1DIM is more difficult to understand. The N(^4S) loss rate is sensitive to the temperature and the molecular oxygen density through reactions (1) and (3). A colder atmosphere yields more N(^4S) at the expense of NO. However, in the calculations shown in Figure 7, we have already adopted the suggestion of *McCoy* [1983] that the atmosphere was colder than suggested by an MSIS model driven by the observed $F_{10.7}$ value of 292. To drive the MSIS inputs to NOX1DIM for Figure 7, we assumed $F_{10.7} = 150$ for both the daily and 81-day averaged values. When we used the actual values, NOX1DIM produced even less N(^4S) than shown in Figure 7. (Note that for the photoionization and dissociation rates we used the actual daily $F_{10.7}$ value of 292 in scaling the EUV and soft X ray flux; however, above 140 km our calculated NO is relatively insensitive to the solar flux.) Using the *McCoy* [1983] assumption, the NOX1DIM NO is in very good agreement with the observed NO suggesting that reactions (1) and (3) are well modeled and that the O_2 and T profiles are not the cause of the overly low calculated N(^4S). The major sources of N(^4S) include the direct photolysis of molecular nitrogen (J_{N2}) and the quenching of N(^2D) by O. In principle, if these terms were dramatically underestimated, the NOX1DIM N(^4S) would also be underestimated. However, we feel it is quite unlikely that either of these terms could be off an amount large enough to yield up to a factor of 10 more N(^4S) at 140 km. Futhermore, such a large increase in N(^4S) at 140 km would cause a large decrease in the calculated NO and thus negate the currently good comparison between measured and model NO that exists at that altitude. We thus do not have a good explanation for the N(^4S) at 140 km.

[21] Figure 8 shows that the disagreement between NOX1DIM N(^4S) with NRLMSIS N(^4S) depends upon

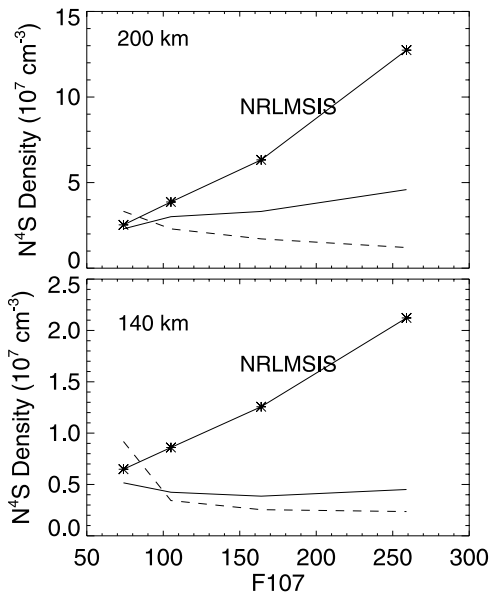

Figure 8. Solar cycle variation of N(^4S) from two NOX1DIM calculations compared with N(^4S) from NRLMSIS for 200 km and 140 km. The dates and location (31°N) are the same as used in Figure 5 (see Table 2). The time is 1500 LT. The solid line with stars is the prediction from NRLMSIS, the solid line without stars is the NOX1DIM N(^4S) using NRLMSIS as input, and the dashed line is the NOX1DIM N(^4S) using MSIS90 as input.

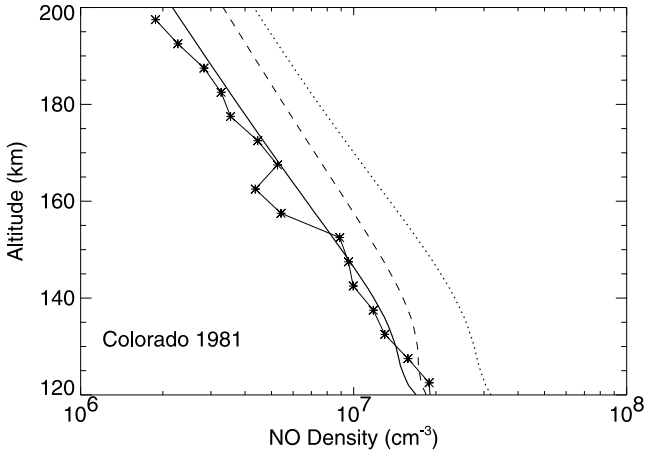

Figure 9. Sensitivity of calculated NO to changes in the reaction rate coefficient for reaction (2). The data are the 1981 Colorado rocket data shown in Figure 4. The solid line uses the value 6×10^{-12} cm^3 s^{-1}, the dashed curve uses the value suggested by *Herron* [1999], and the dotted curve uses the value suggested by *Duff et al.* [2003].

the level of solar activity. The comparison here is for 1500 LT at the location and dates of the Tokyo rocket campaign (although they did not actually measure N(^4S)). Figure 8 shows that at solar minimum, the NOX1DIM results agree with NRLMSIS, but diverge for higher levels of solar activity. As shown in Figure 7, the NOX1DIM N(^4S) depends strongly upon which MSIS model, and thus which O_2, is used as input. This is particularly true at 200 km where the calculated N(^4S) with MSIS90 as input has the opposite solar cycle variation as NRLMSIS. However, even with the NRLMSIS O_2 as an input, the NOX1DIM N(^4S) still shows a large discrepancy with NRLMSIS. As discussed above (compare Figure 7), some of this discrepancy is likely due to an overestimate of the N(^4S) at solar maximum by the empirical model, but some of this discrepancy is also likely due to errors in our theory of atomic nitrogen.

5. Discussion

5.1. Kinetic Uncertainties

[22] Although our results are improved over previous, uncertainties remain due to uncertainties in the kinetic parameters which are used by the photochemical model. Recently, the rate of reaction (2) has received some discussion in the literature. Our calculations assume a temperature-independent value of 6×10^{-12} cm^{-3} s^{-1}. However, in a recent review, *Herron* [1999] has suggested $9.7 \times 10^{-12} e^{-185/T}$ and *Duff et al.* [2003] have recently proposed 6.2×10^{-12} (T/300), based upon a quasiclassical trajectory (QCT) analysis. The difference between these values are important and can affect our results. Figure 9 demonstrates this explicitly. It presents a comparison of three calculated NO profiles (all using NRLMSIS00 as input) with the 1981 Colorado data (e.g., Figure 4). The best comparison is with our assumed temperature-independent reaction rate. The newer proposed rates yield more NO, with the QCT rate yielding a calculated NO that is twice the observations. If the reaction (2) truly is faster at higher temperatures as suggested by *Herron* [1999] and *Duff et al.* [2003], it means that either the O_2 is even lower than that given by NRLMSIS or that some other uncertainty remains in the NO chemical scheme. We should stress that reaction (2) has never been measured at temperatures appropriate for the middle thermosphere.

5.2. Coupling of Atmospheric Layers

[23] Finally, one interesting ramification of the new O_2 data is that it will tend to lower the calculated NO near the peak of the NO layer at 110 km. This is demonstrated in Figure 10 which presents the ratio of two NO calculations. One calculation used MSIS90 as an input, the second used MSIS90 below 120 km and NRLMSIS above 120 km. Thus this comparison serves to illustrate how the effects of neutral composition changes above 120 km can propagate down to lower altitudes. Near 108 km (the peak of the calculated NO), Figure 10 shows the old MSIS90 inputs give a greater NO by up to a factor of 1.2 in the morning hours. The physical mechanism for this effect is the downward diffusion of N(^4S). The higher N(^4S) calculated with the NRLMSIS inputs will cause greater NO loss below 120 km, particularly during the night and early morning hours where chemical NO production is small. Thus the calculation with MSIS90 gives 10–20% more NO at the peak. Although not a dramatic effect, it does serve as an example of vertical coupling and of how uncertainties in the O_2 density profile in the middle thermosphere can effect our estimates of atmospheric composition at lower altitudes.

6. Summary

[24] The NRLMSIS model clearly gives an improved agreement with both NO and N(^4S) data measured from sounding rockets. This offers strong, albeit indirect, validation for the SMM O_2 data of *Aikin et al.* [1993]. Our results

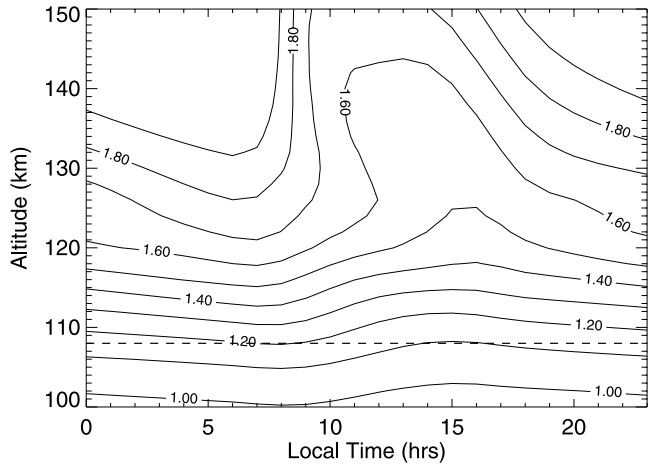

Figure 10. Ratio of NO calculated with MSIS90 to that with a hybrid input that used MSIS90 below 120 km and NRLMSIS above 120 km. Since both calculations used the same input below 120 km, any changes in the NO at those altitudes are effects propagating down from higher altitudes. The horizontal dashed line is a fiducial to indicate the altitude of the peak NO.

are therefore consistent with their argument that O_2 above 140 km is not in diffusive equilibrium and that the timescales for photochemical destruction of O_2 are shorter than diffusive transport. A multidimensional model, such as the TIME-GCM [*Roble and Ridley*, 1994] is needed to physically understand the specific chemical loss rates of O_2 and to assess whether the NRLMSIS O_2 is theoretically valid. Other uncertainties remain in the chemistry of atomic nitrogen, both $N(^2D)$ and $N(^4S)$, particularly for solar maximum conditions.

[25] **Acknowledgments.** Funding for this work has come in part from the Office of Naval Research. We thank Andrew Kochenash of Computational Physics, Inc. for his assistance with the photochemical calculations, David Cleary and Steven Hill for their assistance with the MUSTANG data, and Phil Richards for sharing his preprint with us, which alerted us to the new recommendation for the $N(^2D) + O_2$ reaction rate coefficient.

[26] Arthur Richmond thanks the reviewers for their assistance in evaluating this paper.

References

Aikin, A. C., A. E. Hedin, D. J. Kendig, and S. Drake (1993), Thermospheric molecular oxygen measurements using the ultraviolet spectrometer on the solar maximum mission spacecraft, *J. Geophys. Res.*, *98*, 17,607–17,613.

Bevington, P. R. (1969), *Data Reduction and Error Analysis for the Physical Sciences*, 336 pp., McGraw-Hill, New York.

Bishop, J., and P. D. Feldman (2003), Analysis of the Astro-1/Hopkins Ultraviolet Telescope EUV-FUV dayside nadir spectral radiance measurements, *J. Geophys. Res.*, *108*(A6), 1243, doi:10.1029/2001JA000330.

Bucsela, E. J., D. D. Cleary, K. F. Dymond, and R. P. McCoy (1998), Atomic and molecular emissions in the middle ultraviolet dayglow, *J. Geophys. Res.*, *103*, 29,215–29,228.

Cleary, D. D. (1986), Daytime high-latitude rocket observations of the NO γ, δ, and ϵ bands, *J. Geophys. Res.*, *91*, 11,337–11,344.

Cleary, D. D., S. Gnanalingam, R. P. McCoy, K. F. Dymond, and F. G. Eparvier (1995), The middle ultraviolet dayglow spectrum, *J. Geophys. Res.*, *100*, 9729–9739.

Cravens, T. E. (1981), The global distribution of nitric oxide at 200 km, *J. Geophys. Res.*, *86*, 5710–5714.

DeMore, W. B., S. P. Sander, D. M. Golden, M. J. Molina, R. F. Hampson, M. J. Kurylo, C. J. Howard, and A. R. Ravishankara (1990), Chemical kinetics and photochemical data for use in stratospheric modeling: Evaluation number 9, *Publ. 90-1*, 217 pp., Jet Propul. Lab., Pasadena, Calif.

Duff, J. W., H. Dothe, and R. D. Sharma (2003), On the rate coefficient of the $N(^2D) + O_2 \rightarrow NO + O$ reaction in the terrestrial thermosphere, *Geophys. Res. Lett.*, *30*(5), 1259, doi:10.1029/2002GL016720.

Eparvier, F. G., and C. A. Barth (1992), Self-absorption theory applied to rocket measurements of the nitric oxide (1, 0) γ band in the daytime thermosphere, *J. Geophys. Res.*, *97*, 13,723–13,731.

Hedin, A. E. (1987), MSIS-86 thermospheric model, *J. Geophys. Res.*, *92*, 4649–4662.

Hedin, A. E. (1991), Extension of the MSIS thermosphere model into the middle and lower atmosphere, *J. Geophys. Res.*, *96*, 1159–1172.

Herron, J. T. (1999), Evaluated chemical kinetics data for N and $N_2(A)$ in the gas phase, *J. Phys. Chem. Ref. Data*, *28*, 1453–1483.

Hill, S. M., S. C. Solomon, D. D. Cleary, and A. L. Broadfoot (2000), Temperature dependence of the reaction $N_2(A^3\sum_u^+) + O$ in the terrestrial thermosphere, *J. Geophys. Res.*, *105*, 10,615–10,629.

Iwagami, N., and T. Ogawa (1987), Thermospheric NO profiles observed at the diminishing phase of solar cycle 21, *Planet. Space Sci.*, *35*, 191–198.

Kita, K., N. Iwagami, and T. Ogawa (1988), Thermospheric NO measurement at solar minimum, *J. Geomagn. Geoelectr.*, *40*, 261–268.

Kuze, A., and T. Ogawa (1988), Solar cycle variation of thermospheric NO: A model sensitivity study, *J. Geomagn. Geoelectr.*, *40*, 1053–1065.

McCoy, R. P. (1983), Thermospheric odd nitrogen: 1. NO, $N(^4S)$, $O(^3P)$ densities from rocket measurements of the NO δ and γ bands and the O_2 Herzberg I bands, *J. Geophys. Res.*, *88*, 3197–3205.

Michael, J. V., and K. P. Lim (1992), Rate constants for the N_2O reaction system: Thermal decomposition of N_2O; $N + NO \rightarrow N_2 + O$; and implications for $O + N_2 \rightarrow NO + N$, *J. Chem. Phys.*, *97*, 3228–3234.

Minschwaner, K., J. Bishop, S. A. Budzien, K. F. Dymoond, D. E. Siskind, M. H. Stevens, and R. P. McCoy (2003), Middle and upper thermospheric odd nitrogen: 2. Measurements of nitric oxide from Ionospheric Spectroscopy and Atmospheric Chemistry (ISAAC) satellite observations of NO γ band emission, *J. Geophys. Res.*, *108*, doi:10.1029/2003JA009941, in press.

Ogawa, T., N. Iwagami, and Y. Kondo (1984), Solar cycle variation of thermospheric nitric oxide, *J. Geomagn. Geoelectr.*, *36*, 317–340.

Picone, J. M., A. E. Hedin, D. P. Drob, and A. C. Aikin (2002), NRLMSISE-00 empirical model of the atmosphere: Statistical comparisons and scientific issues, *J. Geophys. Res.*, *107*(A12), 1468, doi:10.1029/2002JA009430.

Roble, R. G., and E. C. Ridley (1994), A thermosphere-ionosphere-mesosphere-electrodynamics general circulation model (time-GCM): Equinox solar cycle minimum simulations (30–500 km), *Geophys. Res. Lett.*, *21*, 417–420.

Roble, R. G., E. C. Ridley, and R. E. Dickenson (1987), On the global mean structure of the thermosphere, *J. Geophys. Res.*, *92*, 8745–8758.

Siskind, D. E., and D. W. Rusch (1992), Nitric oxide in the middle to upper thermosphere, *J. Geophys. Res.*, *97*, 3209–3217.

Siskind, D. E., C. A. Barth, and D. D. Cleary (1990), The possible effect of solar soft X rays on thermospheric nitric oxide, *J. Geophys. Res.*, *95*, 4311–4317.

Siskind, D. E., D. J. Strickland, R. R. Meier, T. Majeed, and F. G. Eparvier (1995), On the relationship between the solar soft X ray flux and thermospheric nitric oxide: An update with an improved photoelectron model, *J. Geophys. Res.*, *100*, 19,687–19,694.

Stevens, M. H. (1995), Nitric oxide γ band fluorescent scattering and self-absorption in the mesosphere and lower thermosphere, *J. Geophys. Res.*, *100*, 14,735–14,742.

Strickland, D. J., J. Bishop, J. S. Evans, T. Majeed, P. M. Shen, R. J. Cox, R. Link, and R. E. Huffman (1999), Atmospheric Ultraviolet Radiance Integrated Code (AURIC): Theory, software architecture, inputs, and selected results, *J. Quant. Spectrosc. Radiat. Transfer*, *62*, 689–742.

Wennberg, P. O., J. G. Anderson, and D. K. Weisenstein (1994), Kinetics of reactions of ground state nitrogen atoms ($^4S_{3/2}$) with NO and NO_2, *J. Geophys. Res.*, *99*, 18,839–18,846.

K. Minschwaner, Department of Physics, New Mexico Institute of Mining and Technology, Socorro, NM 87801, USA. (krm@kestrel.nmt.edu)

J. M. Picone, D. E. Siskind, and M. H. Stevens, E. O. Hulburt Center for Space Research, Naval Research Laboratory, Code 7641, 4555 Overlook Avenue SW, Washington, DC 20375, USA. (picone@nrl.navy.mil; siskind@uap2.nrl.navy.mil; stevens@uap2.nrl.navy.mil)